Japanese Journal of Applied Physics
Vol. 43, No. 5B, 2004, pp. L673–L675
©2004 The Japan Society of Applied Physics

Very Compact Arrayed-Waveguide-Grating Demultiplexer Using Si Photonic Wire Waveguides

Tatsuhiko FUKAZAWA, Fumiaki OHNO and Toshihiko BABA

Department of Electrical and Computer Engineering, Yokohama National University, 79-5 Tokiwadai, Hodogaya-ku, Yokohama 240-8501, Japan

(Received December 16, 2003; accepted March 18, 2004; published April 28, 2004)

We demonstrated an arrayed-waveguide-grating (AWG) demultiplexer using Si photonic wire waveguides, for the first time. We designed and fabricated an AWG of $110 \times 93\,\mu m^2$ size on a silicon-on-insulator substrate. The demultiplexing function was observed in the wavelength range of 1.50–1.57 μm with a channel spacing of ~6 nm and a free spectral range of >90 nm. A narrower channel spacing of 1 nm is possible in an area of $\sim(500\,\mu m)^2$, using an optimization of arrayed waveguides and slab waveguides. [DOI: 10.1143/JJAP.43.L673]

KEYWORDS: photonic wire, SOI, silicon photonics, integrated optics, optical waveguides, AWG, PLC

The silica-based arrayed-waveguide-grating (AWG) demultiplexer is widely used as a key device for wavelength-division-multiplexing (WDM) systems in the 1.5–1.6 μm wavelength range due to its narrow channel spacing, low crosstalk and low insertion loss. Various functionalities such as add/drop multi/demultiplexing, channel selection, and multiwavelength modulation, which are realized by integrating multiple AWGs, are additional attractive features. However, the silica waveguide has a low relative refractive index difference Δ of <1.5%. The smallest AWG still has a size of cm^2 order, as the bend radius allowed for the low-Δ waveguide is larger than 2 mm.[1)] For future WDM systems, it is necessary to reduce the size and increase the integration density of AWGs. An advanced structure is a III-V based AWG with high mesa waveguides.[2)] The waveguide has a standard semiconductor/semiconductor structure in the vertical direction with Δ of ~7%, while it has a semiconductor/air structure in the lateral direction with an ultrahigh Δ of >40%. It allows a bend radius of 100 μm order, which is restricted by the vertical leakage loss at the bend. The total size of the AWG can be of the order of mm square. This size is remarkably small compared with silica ones, but still not sufficiently small as an independent device in a future, more sophisticated functional circuit. In addition, this device requires a complex dry etching process for the formation of 2–3 μm height mesas. Particularly, a high aspect ratio of >20 is ideally required for narrow grooves between neighboring arrayed waveguides in the connection parts with slab waveguides. An insufficient aspect ratio results an excess loss in the transmission characteristics.

The Si photonic wire waveguide (PWW) based on a silicon-on-insulator (SOI) substrate[3–11)] has a Si (refractive index $n \sim 3.5$) rectangular channel core and SiO_2 ($n \sim 1.45$) and/or air claddings. Therefore, an ultrahigh Δ of >40% is maintained in all directions. It allows the marked miniaturization of the bend radius to a few μm. Thus far, a microring filter[3,7,8)] and a lattice filter[9)] have been demonstrated using this waveguide, but no AWG has been reported yet. Here, we do not discuss an AWG with low mesa rib-type waveguides on SOI substrate, since it does not have the advantages of the ultrahigh-Δ waveguide. It rather has size compatibility with silica AWGs, which is beyond the scope of this study. As shown in the following, the μ-bend of the PWW expands the design flexibility of the AWG and allows the marked miniaturization of the total device size to $(100\,\mu m)^2$ order. Since a typical core height of the PWW is 0.3 μm, the etching process is much easier and more precise than that for the high mesa type. In this study, we designed and fabricated such a compact AWG, and observed a clear demultiplexing characteristic in the 1.50–1.57 μm wavelength range.

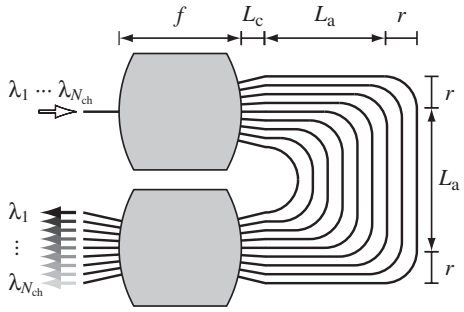

Fig. 1. Schematic of horseshoe-shaped AWG.

We designed a horseshoe-shaped AWG with N arrayed waveguides and two slab waveguides, as shown in Fig. 1. The arrayed waveguides are composed of 90° bends and straight waveguides, and have a constant path length difference ΔL between neighboring waveguides. This configuration is effective for reducing the total device size, compared with a standard V-shape AWG. The device size S excluding input and output waveguides is approximated by

$$S \approx (L_a + L_c + f + r) \cdot (2r + L_a), \tag{1}$$

where L_a denotes one third of the outermost length of the arrayed waveguides, which is roughly expressed as $(N-1)\Delta L/3$, L_c is the distance between the arrayed waveguides and the slab waveguide, and r is the bend radius. The channel spacing $\Delta\lambda$ is expressed as[12)]

$$\Delta\lambda = n_{slab} d D \lambda_0 / n_g f \Delta L, \tag{2}$$

where n_{slab} is the equivalent modal index of the slab waveguide, n_g is the group index of the arrayed waveguides, d and D are the pitches of the arrayed waveguides and of the output waveguides at the connection part with the slab waveguides, respectively, λ_0 is the center wavelength of channels, and f is the focal length of the slab waveguides. The path length difference ΔL is designed with the diffraction order m as[12)]

$$\Delta L = m\lambda_0 / n_{eq}, \tag{3}$$

where n_{eq} is the equivalent modal index of the arrayed waveguides. Let us assume the parameters shown in Table I. Indexes n_{slab} and n_{eq} in Table I are typical values for the

Table I. Design parameters for device size estimation.

Parameter	Symbol	Value
Center wavelength	λ_0	1550 nm
Number of arrayed waveguide	N	34
Arrayed waveguides separation	d	0.75 μm
Output waveguides separation	D	0.75 μm
Bend rudius of arrayed waveguides	r	5 μm
Connection length	L_c	10 μm
Slab index	n_{slab}	3.06
Equivalent modal index	n_{eq}	2.692
Group index	n_g	4.5

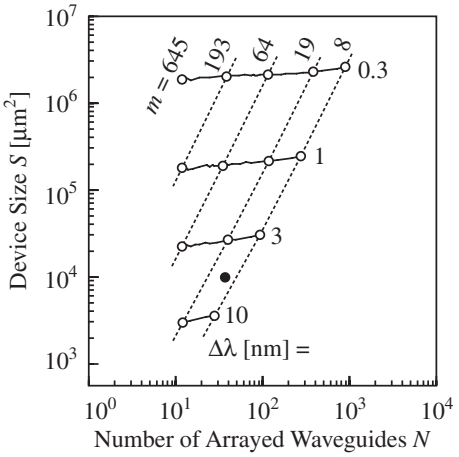

Fig. 2. Device size versus number of arrayed waveguides. Black circle denotes the design in the experiment.

PWW. The large group index n_g, which arises from a large structural dispersion,[4] is effective for the shortening of arrayed waveguides. Using (1)–(3), the device size S is roughly estimated as a function of the number of the arrayed waveguides N as shown in Fig. 2. Here, N and S are determined so that the sidelobe level of demultiplexed light is less than -50 dB after the fine tuning of the light intensity distribution in the arrayed waveguides. The order m is chosen to be larger than seven to prevent coupling between neighboring waveguides. The focal length f is flexibly changed so that the target channel spacing is achieved according to (2). The total size is mainly determined not by N but ΔL because there is a tradeoff relation between N and f against the requirement for the sidelobe level. For $\Delta\lambda = 3$ nm and 0.3 nm at $\lambda_0 = 1.55$ μm, the minimum device sizes are $(150\,\mu m)^2$ and $(1.4\,mm)^2$, respectively.

In the experiment, we used a unibond-type SOI substrate with a Si layer of 0.32 μm thickness and an SiO_2 layer of 1.0 μm thickness. The device was formed by electron beam lithography and CF_4 based inductively coupled plasma etching. The details of the fabrication process are similar to those described in ref. 4. The width of each channel waveguide was 0.35 μm, which satisfies the single mode condition at $\lambda = 1.55$ μm. Figure 3 shows a fabricated device of $100 \times 93\,\mu m^2$ size excluding the input and output waveguides. Parameters for a target channel spacing of 3 nm in this experiment are summarized in Tables I and II. The device size is slightly smaller than that predicted from

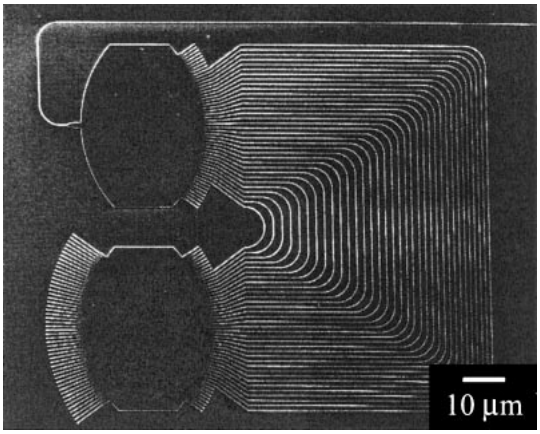

Fig. 3. Scanning electron micrograph of fabricated AWG.

Table II. Design parameters for fabricated device.

Parameter	Symbol	Value
Diffraction order	m	10
Path length difference	ΔL	5.8 μm
Slab focal length	f	30 μm
Device size	S	$110 \times 93\,\mu m^2$

Fig. 2, since the requirement for the sidelobe level was relaxed in this design. A half-elliptical taper[10] of $3.5 \times 1.5\,\mu m^2$ was placed between the input waveguide and the slab waveguide to smoothly excite a Gaussian beam in the slab waveguide. Similarly, $1.5\,\mu m \times 0.8\,\mu m$ tapers were placed between the slab waveguides and other channel waveguides to reduce the joint loss. Each pair of elliptical tapers was separated by grooves of ~10 nm end width. The nonuniformity in width of the arrayed waveguides was less than ±2% (the resolution limit of the field-emission-type scanning electron microscope used, JEOL JSM-6700F). The output waveguides were terminated inside the substrate. In the measurement, light from a tunable laser system was focused at the cleaved facet of the input waveguide by a pair of objective lenses. Light output from each end of the output waveguide was observed by a vidicon camera and measured by an optical power meter. During the measurement, the facet was shadowed from undesired light by a field stop. Figure 4 shows the transmission spectra for TE-polarized

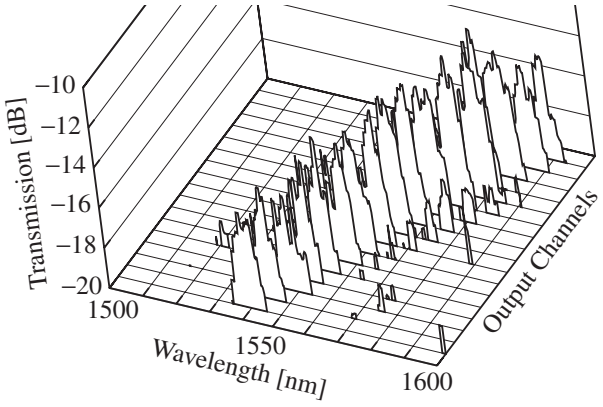

Fig. 4. Transmission spectra for 17 output waveguides.

input light. Here, the vertical axis excludes input and output coupling losses between the device and the measurement setup, which were evaluated separately. The clear spectral peak appeared and shifted linearly among the 17 output waveguides. The fine structure in the peak was caused by the Fabry-Perot resonance inside the device. This resonance can be suppressed by further optimizing the tapers and adding an anti-reflection coating or a spot-size converter at the waveguide ends.[11] The peak interval was 3 nm, which well agreed with the designed value. However, the full width at half maximum (FWHM) of each peak was ~6 nm. Therefore, the number of fully separated channels was nine. The sidelobe level was nearly −5 dB of the main peak intensity. The FWHM and the sidelobe level can be improved by optimizing the tapers and the focal length f to form a high-quality Gaussian beam in the slab waveguides, and also by reducing the nonuniformity of arrayed waveguides to maintain a smooth wavefront. In each spectrum, no other main peaks were observed over the measured wavelength range of 100 nm. The free spectral range (FSR) was wider than 90 nm.

In conclusion, we designed and fabricated an AWG within $\sim(100\,\mu\mathrm{m})^2$ area by using Si PWWs on an SOI substrate, and experimentally demonstrated the demultiplexing function for nine channels with a spacing of ~6 nm and an FSR of >90 nm. Such a very compact AWG will greatly simplify the dense integration of multiple AWGs for more sophisticated functions.

This work was supported by the IT Program and the 21st Century COE Program of MEXT, and CREST #530-13 of JST.

1) For example, M. Ishii,Y. Hibino, Y. Hida, A. Kaneko, M. Itoh, T. Goh, A. Sugita, T. Saida, A. Himeno and Y. Ohmori: European Conf. Opt. Commun. **3** (2000) 27.
2) M. Kohtoku, H. Sanjoh, S. Oku, Y. Kadota, Y. Yoshikuni and Y. Shibata: Electron. Lett. **33** (1997) 1786.
3) B. E. Little, J. S. Forsi, G. Steinmeyer, E. R. Thoen, S. T. Chu, H. A. Haus, E. P. Ippen, L. C. Kimerling and W. Greene: IEEE Photonics Technol. Lett. **10** (1998) 549.
4) A. Sakai, G. Hara and T. Baba: Jpn. J. Appl. Phys. **40** (2001) L383.
5) A. Sakai, T. Fukazawa and T. Baba: IEICE Trans. Electron. **E85-C** 1033 (2002) 1033.
6) T. Fukazawa, A. Sakai and T. Baba: Jpn. J. Appl. Phys. **41** (2002) L1461.
7) A.Vörckl, M. Mönster, W. Henschel, P. H. Bolivvar and H. Kurz: IEEE Photonics Technol. Lett. **15** (2003) 921.
8) P. Dumon, W. Bogaerts, J. V. Campenhout, V. Wiaux, J. Wouters, S. Beckx and R. Baets: Annual Meet. Laser and Electro-Optics Soc. **1** (2003) 289.
9) K. Yamada, T. Shoji, T. Tsuchizawa, T. Watanabe, J. Takahashi and S. Itabashi: Opt. Lett. **28** (2003) 1663.
10) T. Fukazawa, T. Hirano, F. Ohno and T. Baba: Jpn. J. Appl. Phys. **42** (2004) 646.
11) T. Shoji, T. Tsuchizawa, T. Watanabe, K. Yamada and H. Morita: Electron. Lett. **38** (2002) 1669.
12) K. Okamoto: *Fundamentals of Optical Waveguides*, eds. P. L. Kelley, I. P. Kaminow and G. P. Agrawal (Academic Press, San Diego, 2000) Chap. 9.